NEUROSCIENCE
INTERNATIONAL BRAIN IBRO RESEARCH ORGANIZATION
RESEARCH ARTICLE
G. Wang et al. / Neuroscience xxx (2023) xxx–xxx

Neural Representation of Collective Self-esteem in Resting-state Functional Connectivity and its Validation in Task-dependent Modality

Guangtong Wang, [†] **Mei Zeng** [†] **Jiwen Li Yadong Liu, Dongtao Wei, Zhiliang Long, Haopeng Chen, Xinlei Zang and Juan Yang** [*]

Faculty of Psychology, Southwest University, Chongqing 400715, China

Key Laboratory of Cognition and Personality, Ministry of Education, Southwest University, Chongqing 400715, China

Abstract—*Introduction:* Collective self-esteem (CSE) is an important personality variable, defined as self-worth derived from membership in social groups. A study explored the neural basis of CSE using a task-based functional magnetic resonance imaging (fMRI) paradigm; however, task-independent neural basis of CSE remains to be explored, and whether the CSE neural basis of resting-state fMRI is consistent with that of task-based fMRI is unclear.

***Methods:* We built support vector regression (SVR) models to predict CSE scores using topological metrics measured in the resting-state functional connectivity network (RSFC) as features. Then, to test the reliability of the SVR analysis, the activation pattern of the identified brain regions from SVR analysis was used as features to distinguish collective self-worth from other conditions by multivariate pattern classification in task-based fMRI dataset.**

***Results:* SVR analysis results showed that leverage centrality successfully decoded the individual differences in CSE. The ventromedial prefrontal cortex, anterior cingulate cortex, posterior cingulate gyrus, precuneus, orbitofrontal cortex, posterior insula, postcentral gyrus, inferior parietal lobule, temporoparietal junction, and inferior frontal gyrus, which are involved in self-referential processing, affective processing, and social cognition networks, participated in this prediction. Multivariate pattern classification analysis found that the activation pattern of the identified regions from the SVR analysis successfully distinguished collective self-worth from relational self-worth, personal self-worth and semantic control.**

***Conclusion:* Our findings revealed CSE neural basis in the whole-brain RSFC network, and established the concordance between leverage centrality and the activation pattern (evoked during collective self-worth task) of the identified regions in terms of representing CSE.**

Key words: Collective self-esteem, Orthogonal minimal spanning trees, Graph analysis, Multivariate pattern analysis.

INTRODUCTION

Self-esteem has been studied by psychologists for many decades (James et al., 1890). Recently, with the development of the social identity theory, collective self-esteem (CSE) has gradually gained increasing attention in the field of self-esteem. CSE refers to self-worth derived from membership in social groups (Crocker & Major, 1989; Luhtanen & Crocker, 1992), emphasizing the influence of a group on self-concept. Researchers have found that CSE has an important effect on maintaining an individual's mental health. Specifically, people with high CSE have been shown to exhibit modestly higher subjective well-being and life satisfaction scores (Crocker et al., 1994; Bettencourt et al., 1999), while those with low CSE are at an increased risk of psychiatric disorders such as anxiety and depression (Hassan et al., 2013).

Previous studies have used self-report scales and cognitive neuroscience techniques to explore CSE (Crocker et al., 1994; Du, King, & Chi, 2017; Chen et al., 2021a,b; Zeng et al., 2021). By measuring the neural signals when subjects performed a collective self-worth task during functional magnetic resonance imaging (fMRI), a previous study facilitated a preliminarily understanding of the neural basis of CSE (Zeng et al., 2021); this study found that the cortical midline structure

[*]Correspondence to: Juan Yang, Faculty of Psychology, Southwest University, Chongqing 400715, China.
E-mail address: valleyqq@swu.edu.cn (J. Yang).

[†] These authors equally contributed to this work.
Abbreviations: CSE, collective self-esteem; fMRI, functional magnetic resonance imaging; SVR, support vector regression; RSFC, resting-state functional connectivity network; IPL, inferior parietal lobule; TPJ, temporoparietal junction; MVPA, multivariate pattern analysis.

https://doi.org/10.1016/j.neuroscience.2023.08.017
0306-4522/

(CMS), parahippocampal gyrus, anterior insula, posterior insula, caudate, postcentral gyrus, inferior parietal lobule (IPL), and temporoparietal junction (TPJ) were involved in CSE processing. Specifically, the CMS, which is known to play a role in self-referential evaluation processing (Northoff et al., 2006), was found to be involved in retrieving group-related memories and making value assessments during CSE processing. In addition, the posterior insula and postcentral gyrus were engaged in generating appropriate emotional responses in association with CSE processing. Further, the TPJ and IPL were engaged in the process of inferring the attitudes of others outside the group towards their group from a third-person perspective (Premack & Woodruff, 1978; Frith & Frith, 2005; Van Overwalle & Baetens, 2009).

However, prior studies focused only on a task-based paradigm, which might be heavily dependent on the self-worth paradigm and experimental materials used to induce CSE (Zeng et al., 2021). This approach neglects the general neural representation for individual differences in CSE. Moreover, self-esteem is usually considered a personality trait that is relatively stable and affects long-term behavioral style regardless of specific situations (Jaccard, 1974; Neiss et al., 2002; Furr, 2009). Therefore, it is necessary to explore the task-independent neural basis of CSE.

Compared with task-based fMRI, resting-state fMRI provides a different perspective to understand brain function (Lacosse et al., 2021). It has been suggested that the features of resting-state functional connectivity (RSFC) can predict task-based activation maps (Cole et al., 2016; Tavor et al., 2016; Jones et al., 2017; Tobyne et al., 2018; Osher et al., 2019). As such, RSFC patterns correspond to task-based co-activation patterns (Krienen et al., 2014). However, it is still unknown whether concordance exists between RSFC pattern and the activation pattern during a collective self-worth task in terms of representing CSE.

Advances in brain imaging analysis techniques have provided a new avenue to explore spontaneous brain activity signals. RSFC has served as a “fingerprint” for identifying individual differences (Tang et al., 2013; Finn et al., 2015; Dubois et al., 2018; Nostro et al., 2018; Kashyap et al., 2019; Passamonti et al., 2019; Altinok et al., 2021). The results from RSFC studies are very dependable, with high test–retest reliability if there is sufficient sample data (Cao et al., 2014; Zuo & Xing, 2014; Noble et al., 2017). Decoding the individual differences in self-esteem using seed-based RSFC analysis has been attempted previously (Chavez & Heatherton, 2015; Pan et al., 2016; Kawamichi et al., 2018; Chen et al., 2021a, b). However, these studies mainly focused on the functional synchrony between two specific brain regions. The potential use of whole-brain RSFC analysis in uncovering more subtle individual differences compared to any local or seed-based RSFC analyses has been demonstrated (Liu et al., 2019). As such, the topological metrics (e.g., nodal betweenness centrality) extracted from whole-brain RSFC networks have been widely used to predict multiple psychological constructs, such as the five-factor model personality traits (Toschi et al., 2018; Kong et al., 2019), chronic insomnia disorder (Li et al., 2018), Alzheimer’s disease (Hojjati et al., 2017), depression (Onoda & Yamaguchi, 2015), and consciousness (Uehara et al., 2014). Graph analysis can quantitatively depict the organizational principles of complex brain networks (Bullmore & Sporns, 2009). It has consistently been demonstrated that the topological metrics of RSFC networks successfully detect subtle individual differences (Deng et al., 2016; Liu et al., 2017; Feng et al., 2018a,b; Tang et al., 2018). Therefore, utilizing topological metrics for quantitatively depicting whole-brain RSFC networks is warranted.

Moreover, an increasing number of neuroimaging studies have employed multivariate methods to detect task-based brain activation signals (Woo et al., 2017; Weaverdyck et al., 2020). Instead of detecting the activation strength of a single brain region or voxel in univariate analysis, multivariate pattern analysis (MVPA) depicts spatially distributed patterns of neural activity (Haxby et al., 2001). This improves the sensitivity of detecting subtle differences in psychological or cognitive states (Sapountzis et al., 2010; Jimura & Poldrack, 2012). Previous studies have demonstrated the potential of MVPA to predict self-esteem (Izuma et al., 2018; Li et al., 2021; Zeng et al., 2021). As such, applying MVPA to explore the concordance between RSFC pattern and the activation pattern during collective self-worth task in terms of representing CSE is required.

Overall, the current study aimed to uncover the task-independent neural basis of CSE using graph analysis and machine learning algorithms. Then, to test the reliability of these resting-state analyses, we studied the concordance between RSFC pattern and the activation pattern during a collective self-worth task in terms of representing CSE using multivariate pattern classification analysis. If the activation pattern of the identified brain regions from resting-state analyses can classify collective self-worth and other conditions, the previous resting-state analyses are valid. We speculated that the CMS, posterior insula, caudate, postcentral gyrus, IPL, and TPJ might participate in the prediction of CSE in the resting-state fMRI dataset. Based on the linkage between task-evoked activation maps and RSFC features, we predicted that the activity pattern of the identified regions from resting-state analyses could successfully distinguish collective self-worth condition from other conditions in the task-based fMRI dataset.

EXPERIMENTAL PROCEDURES

Exploring the task-independent neural basis of CSE

First, all participants completed self-report questionnaires. Then, each participant underwent resting-state fMRI scanning. All participants were instructed to close their eyes and not fall asleep or think about anything. Finally, topological metrics from the RSFC networks were extracted and used as features to predict CSE scores. The entire data analysis process is shown in Fig. 2.

Please cite this article in press as: Wang G et al. Neural Representation of Collective Self-esteem in Resting-state Functional Connectivity and its Validation in Task-dependent Modality. Neuroscience (2023), https://doi.org/10.1016/j.neuroscience.2023.08.017

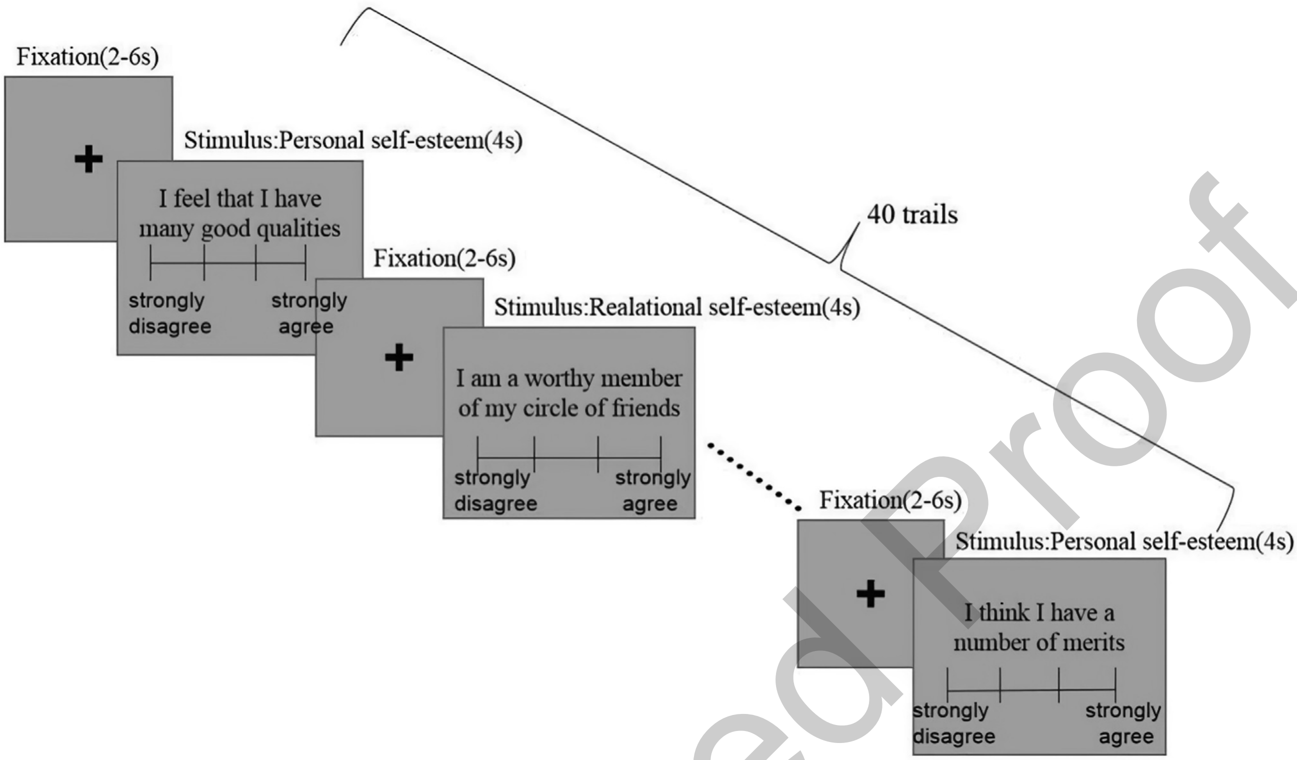

Fig. 1. Illustration of an example run. There are four conditions (collective self-worth, relational self-worth, personal self-worth, and semantic control) in each run. Each condition comprise ten trails. During each trial, a sentence is shown for 4 s followed by a fixation cross that was presented for 2, 4, or 6 s.

Participants. We recruited 249 healthy Chinese undergraduate students from a local university in China who underwent resting-state fMRI data collection. Of these, 23 were excluded due to large head movements (maximal displacement > 2.5 mm, n = 14), extreme measure scores (n = 1), and abnormal functional connectivity (n = 8). Finally, data from 226 participants were included in the resting-state dataset (129 females; age range, 17–24 years; mean age ± standard deviation [SD] = 20.2 ± 1.5 years).

Questionnaire. The Collective Self-Esteem Scale was used to assess collective self-esteem (Luhtanen & Crocker, 1992). The Chinese Revised Collective Self-Esteem Scale contains 16 items that are divided into four dimensions, namely membership esteem (e.g., "I am a valuable member of the social group"), private CSE (e.g., "I feel good about being a member of the group"), public CSE (e.g., "Overall, my social groups are considered good by others"), and importance of identity (e.g., "The social groups I belong to are an important reflection of who I am"). Further, each dimension comprises four items and all are written in Mandarin Chinese. Participants answered these items on a seven-point Likert scale ranging from one (strongly disagree) to seven (strongly agree). The mean values of the 16 items were used for prediction analysis. A prior study containing 420 samples found that the internal consistency coefficient of the Chinese Revised Collective Self-Esteem Scale was 0.84 (Jia, 2009).

Functional neuroimaging data acquisition. The brain imaging data was obtained by a 3 T Prisma Siemens Trio MRI scanner. Resting-state fMRI data was collected with the following echo-planar pulse sequence: repetition time = 2000 ms, echo time = 30 ms, flip angle = 90°, voxel size = 3 × 3 × 3 mm^3, field of view = 192 × 192 mm^2, number of slices = 32, slice thickness = 3 mm, and slice gap = 0.99 mm. The anatomical scan information can be seen in Method S1.1 in the supplementary materials.

Resting-state fMRI data preprocessing. Preprocessing of the resting-state fMRI data was completed using the Data Processing Assistant for resting-state fMRI (DPARSF, https://rfmri.org/dparsf; Yan & Zang, 2010). First, the initial ten volumes were removed to obtain a stable signal, and the remaining 232 volumes were included in the final analysis. The purpose of this step was to avoid unstable signals when the fMRI scanner was turned on but the participants were not ready. Second, slice timing and head motion correction were performed, and the head movement parameters of each participant were obtained. We excluded 14 participants who had a head motion maximal displacement greater than 2.5 mm. Next, we co-registered the functional image to the anatomical image and segmented it into gray matter, white matter, and cerebrospinal fluid. Then, we normalized the functional images onto the standard T1 Montreal Neurological Institute template image with a voxel size of 3 × 3 × 3 mm^3. The functional images were

Please cite this article in press as: Wang G et al. Neural Representation of Collective Self-esteem in Resting-state Functional Connectivity and its Validation in Task-dependent Modality. Neuroscience (2023), https://doi.org/10.1016/j.neuroscience.2023.08.017

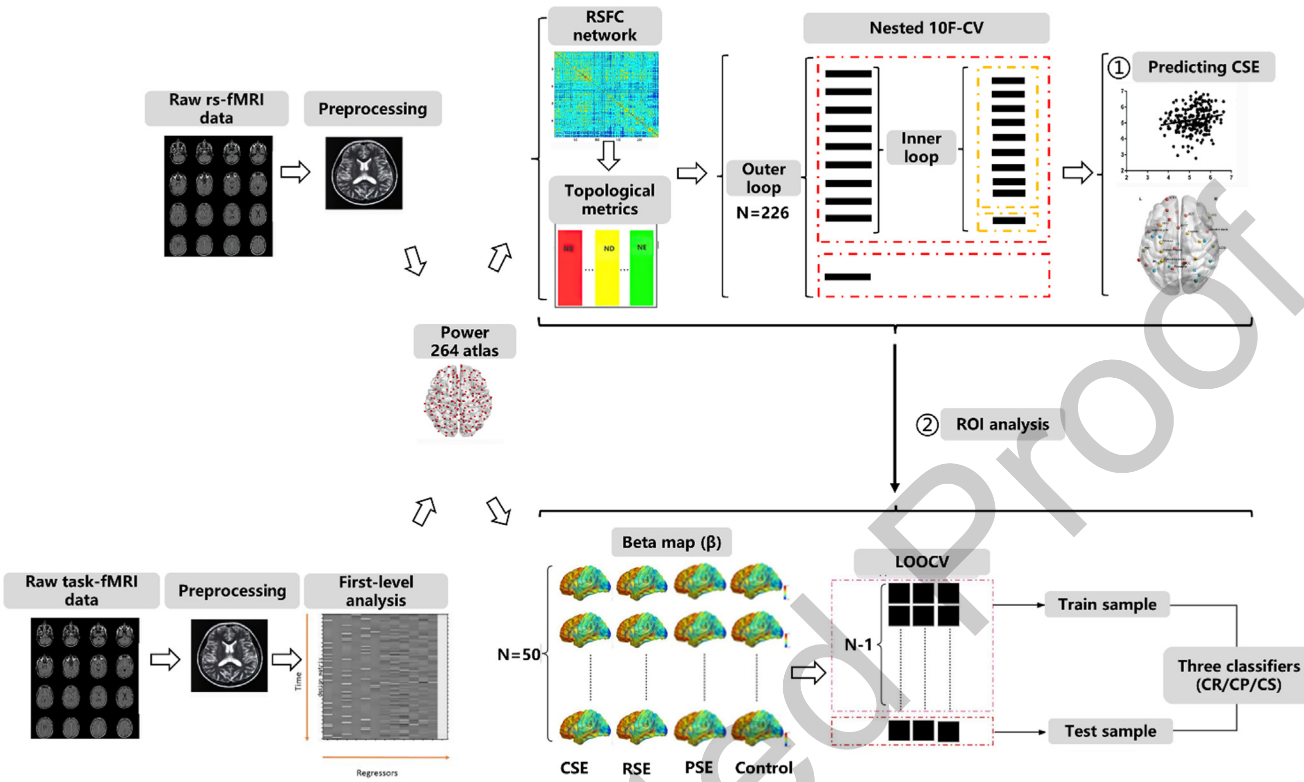

Fig. 2. The overall data analysis procedure. The procedure includes ① predicting collective self-esteem questionnaire scores using graph analysis in resting-state fMRI and ② classifying collective self-worth and three other conditions in task-based fMRI; CP classifier, distinguished collective self-worth from personal self-worth processing; CR classifier, distinguished collective self-worth from relational self-worth processing; CS classifier, distinguished collective self-worth from semantic processing.

smoothed by a 6-mm full-width at half-maximum Gaussian kernel. Subsequently, we used the GRETNA toolbox to perform further preprocessing (https://www.nitrc.org/projects/gretna; Wang et al., 2015). The linear trends were removed, and a temporal band-pass filter (0.009–0.1 Hz) was used to remove low or high-frequency noise and artifacts (Biswal et al., 1995; Zuo et al., 2010). Finally, the effects of redundant parameters (24 movement parameters, white matter signals, and cerebrospinal fluid signals) were regressed.

Graph analysis and support vector regression (SVR). The GRETNA toolbox was used to perform graph analysis wherein RSFC networks were divided into nodes and edges and were filtered by orthogonal minimal spanning trees (Bullmore & Sporns, 2009; Song et al., 2015; Wang et al., 2015; Dimitriadis et al., 2017). Then, SVR models were trained to predict CSE scores.

Network construction. Whole-brain network nodes were defined based on the power-264 atlas that includes 264 non-overlapping 3-mm-radius spheres. The power-264 atlas spans the cerebral cortex, subcortical structures, and cerebellum (Power et al., 2011). The network coordinate of each sphere is registered to the Montreal Neurological Institute space. The parcellation scheme of the power-264 atlas is different from that of the Schaefer atlas regarding the shape and number of spheres (Schaefer et al., 2018). Then, we averaged the blood oxygenation level dependent signals of all the voxels in each region at each time point and calculated the correlation coefficients between all paired regions to build edges, resulting in a 264 × 264 FC matrix for each participant. Then, Fisher-Z transformation was applied to each RSFC matrix.

Network analysis. A thresholding scheme based on orthogonal minimal spanning trees was used to filter the binarized and positive RSFC networks (Dimitriadis et al., 2017; Adamovich et al., 2022). Next, ten different kinds of topological metrics were calculated: betweenness centrality, degree centrality, nodal efficiency, closeness centrality, clustering coefficients, eigenvector centrality, leverage centrality, local efficiency, shortest path length, and subgraph centrality. Betweenness centrality refers to each node's contribution to the shortest path between all other node pairs (He & Evans, 2010). Degree centrality is the number of edges directly connected to each node (Freeman, 1978). Nodal efficiency is the average value of the inverse of the shortest path length between a given node and all other nodes in the network (Boccaletti et al., 2006). Closeness centrality is the closeness between a node and other nodes in the graph (Okamoto et al., 2008). Clustering coefficient reflects the degree of node clustering (Saramäki et al., 2007). Eigenvector centrality measures the influence of each node in the network (Bonacich, 2007). Leverage centrality measures the relationship between the degree of each node and that of their neighbors (Joyce et al., 2010). Local efficiency measures the average global efficiency of the subgraph induced by the neighbors of a node (Latora & Marchiori, 2001). The shortest path length measures the maximal shortest path length that each node has with other nodes in the graph (Chen et al., 2011). Subgraph centrality measures the number of closed loops starting and ending at each node (Estrada & Rodriguez-Velazquez, 2005). A previous study found that the hubs from different metrics could be categorized into connector (e.g., eigenvector centrality), distributed (e.g., degree centrality), and aggregated groups (Wang et al., 2018). They had distinctive characteristics to support their distinguished roles, such as space distribution, topological vulnerability, and cognitive flexibility.

SVR analysis. A linear SVR model with a cost parameter (C) was trained using topological metrics as features in the Libsvm toolbox in MATLAB (https://www.csie.ntu.edu.tw/~cjlin/libsvm). Similar to a previous study (He et al., 2021), nested 10-fold cross-validation (10F-CV) was applied to determine the optimal C (searching in [0.1, 10] with a step of 0.1; Brereton & Lloyd, 2010). The inner 10F-CV determined the optimal C, and the outer 10F-CV estimated the generalization of this model. Specifically, 226 subjects were randomly divided into ten folds; one-fold (10% of subjects) was used as the testing set, and the remaining nine folds (90% of subjects) were used as the training set. Since feature selection may lose some information (Liu et al., 2015) and the feature dimensions (264) were acceptable, each topological metric for each participant was used as features (226 people $\times$ 264 regions) to train a SVR model. Each feature was linearly scaled to the range of 0–1 across the training set to avoid adverse effects caused by the difference in the numeric ranges (Cui & Gong, 2018). Then, the test set was scaled according to the same scaling parameters. The SVR model was built to fit topological metric and CSE scores in the training set and to obtain regression weights for the 264 regions (see Method S1.2 in the supplementary materials). The predicted CSE scores were obtained by feeding the test set to the established SVR model. The ten folds were accomplished before we obtained the predicted CSE scores for each subject and ten weight maps. To achieve robust estimates, we repeated the abovementioned pipeline ten times to calculate the average of the ten predicted CSE scores for each subject. The prediction performance of the model was estimated by Pearson's correlation coefficients and the mean absolute error between the measured and predicted scores. Next, we randomly permutated the measured scores of CSE 1,000 times and placed them into the abovementioned pipeline to obtain a null distribution of correlation coefficients between the measured and predicted scores to evaluate the significance (set at $p < 0.05$). Finally, we averaged 100 weight maps (10-fold $\times$ 10 times) to perform feature selection. Studies have shown that the absolute value of regression weight is able to quantify the predictive contribution of each feature (Dosenbach et al., 2010; Cui et al., 2018). The feature, with a value greater than the mean + 1 SD, was selected from the averaged weight map (Ecker et al., 2010). Moreover, multi-feature combination analysis and prediction of personal and relational self-esteem scores were executed (see Methods S1.3 and S1.4 in the supplementary materials).

Relevance vector regression. To test the robustness of the SVR, relevance vector regression (RVR) was applied (He et al., 2021). RVR adopts Bayesian inference to obtain parsimonious solutions with low computational cost and favorable generalization (Tipping, 2001). As RVR has no algorithm-specific parameter, 10F-CV without nested structure was applied (see Method S1.5 in the supplementary materials).

Validation analysis of task-based fMRI data

To verify the SVR analysis results, some task-based fMRI data was collected. During task-state fMRI scanning, participants completed a self-worth task. This dataset has been used previously to study the neural mechanisms of personal, relational, and collective self-esteem (Zeng et al., 2021). The rationale of this validation analysis is that if the activation patterns of the regions identified (46 regions) in the SVR analysis can distinguish collective self-worth from personal self-worth, relational self-worth and semantic control conditions, the SVR analysis is valid and the identified regions are unique to collective self-esteem. The entire data analysis process is shown in Fig. 2.

Participants. There were 55 participants in the task-state dataset (28 females; aged 18–24 years; mean age ± SD = 20.16 ± 1.50 years); notably, 46 of these participants are in the resting-state dataset. Each participant reported normal or corrected vision and no history of neurological or mental illness, head injury, or drug abuse. This experiment was approved by the Ethics Committee of Southwest University (China), and all participants signed an informed consent form before the experiment.

Self-worth task. The self-worth task contained four fMRI scan runs, and each run was made up of four conditions that included personal self-worth, relational self-worth, collective self-worth, and semantic control. Further, each condition had ten trials in each run. In each trial, subjects viewed a sentence and then evaluated how much they agreed with it on a four-point Likert scale, ranging from one (strongly disagree) to four (strongly agree) (Fig. 1). The collective self-worth stimuli, such as "I feel good about the social groups I belong to," were adapted from the Collective Self-Esteem Scale (Luhtanen & Crocker, 1992). The relational self-worth stimuli, such as "In general, I am glad to be a member of my circle of friends," were adapted from the relational self-esteem scale (Du et al., 2012). The personal self-worth stimuli, such as "I feel that I am a person of worth," were adapted from the Rosenberg Self-Esteem Scale (Rosenberg, 1965). The semantic control stimuli, such as "China is the country with the largest population in the world," was common sense knowledge.

Functional neuroimaging data acquisition. The brain imaging data was obtained by a 3 T Prisma Siemens Trio MRI scanner. Task-based fMRI data was collected with the following echo-planar pulse sequence: repetition time = 2000 ms, echo time = 30 ms, voxel size = $3 \times 3 \times 3\ mm^3$, field of view = $192 \times 192\ mm^2$, number of slices = 32, slice thickness = 3 mm, slice gap = 0.99. The anatomical scan information can be seen in Method S1.1 in the supplementary materials.

Task-based fMRI data preprocessing and first-level analysis. DPARSF was used for the preprocessing of task-fMRI data. First, we removed the initial five volumes. Then, slice timing and realignment were performed to correct slice order and head motion. Next, we co-registered the fMRI data to the anatomical image and segmented it into gray matter, white matter, and cerebrospinal fluid. We then normalized the functional images onto the standard T1 Montreal Neurological Institute template image with a voxel size of $3 \times 3 \times 3\ mm^3$. Finally, we smoothened the functional images with a 6-mm full-width at half-maximum Gaussian kernel. The general linear model in SPM12 (http://www.fil.ion.ucl.ac.uk/spm) was used for first-level analysis and was made up of four conditions (collective self-worth, relational self-worth, personal self-worth, and semantic control) and six movement parameters. This analysis used a high-pass temporal filter with a 128 s cutoff period. The normalized beta estimate was calculated in the four conditions for further pattern-information analysis (Haxby et al., 2001; Li et al., 2021; Zeng et al., 2021).

Multivariate pattern classification. Multivariate pattern classification was performed in three steps, including extraction of beta maps, model building, and interpretation of results.

Extraction of beta maps. The power 264-region atlas was used to construct beta maps. Beta values derived from each voxel in each ROI were averaged, resulting in 264 averaged beta values per condition per participant. The beta maps of the (46) identified regions from the SVR analysis would be used as classification features in the next step.

Model building. Three linear support vector classifiers were built using the LIBSVM toolbox (collective self-worth VS relational self-worth, collective self-worth VS personal self-worth, collective self-worth VS semantic control; http://www.csie.ntu.edu.tw/~cjlin/libsvm/). The parameters were set to default values (C = 1). The leave-one-subject-out cross-validation (LOOCV) procedure was performed to check the generalizability of the model (Cawley & Talbot, 2004; Kaplan et al., 2015). Specifically, in each iteration, one subject was the test set, and the others were the training set. The model trained on the training set was used to predict the test set. The LOOCV program ended after each subject had served as the test set.

Interpretation of results. Receiver operating characteristic (ROC) curves were drawn to describe the classification performance (Vilares et al., 2017; Chow et al., 2018). The area under the curve (AUC) is a widely recognized metric for measuring the classification performance of a machine learning algorithm. The AUC usually ranges from 0.5 to 1, where 1 means the model has perfect classification performance and 0.5 indicates that the classification task was done randomly with a poor classification performance.

RESULTS

The resting-state neural basis of CSE

Behavioral results. The average CSE score of the 226 participants was 5.29, with a SD of 0.62.

Support vector regression results. Prediction of each topological metric. Results showed that leverage centrality ($r = 0.1505$, $p_{pt} = 0.050$, mean absolute error = 0.53, $R^2 = 0.3185$) significantly predicted the measured CSE scores. (Fig. 3). However, nodal betweenness centrality ($r = 0.0546$, $p_{pt} = 0.241$, mean absolute error = 0.54), nodal degree centrality ($r = 0.0582$, $p_{pt} = 0.225$, mean absolute error = 0.53), nodal efficiency ($r = -0.0117$, $p_{pt} = 0.482$, mean absolute error = 0.53), closeness centrality ($r = 0.0138$, $p_{pt} = 0.372$, mean absolute error = 0.52), clustering coefficient ($r = -0.0773$, $p_{pt} = 0.776$, mean absolute error = 0.55), eigenvector centrality ($r = -0.2643$, $p_{pt} = 0.995$, mean absolute error = 0.56), local efficiency ($r = -0.1033$, $p_{pt} = 0.846$, mean absolute error = 0.57), shortest path length ($r = -0.0126$, $p_{pt} = 0.492$, mean absolute error = 0.53), and subgraph centrality ($r = -0.1943$, $p_{pt} = 0.996$, mean absolute error = 0.52) could not significantly predict the measured CSE scores.

In the prediction of leverage centrality, 46 regions were above the threshold (Fig. 3 and Table 1), which were derived from the anterior cingulate cortex (ACC), TPJ, dorsomedial prefrontal cortex (dmPFC), posterior cingulate cortex (PCC), inferior frontal gyrus (IFG), ventromedial prefrontal cortex (vmPFC), middle frontal gyrus (MFG), dorsolateral prefrontal cortex (dlPFC), posterior insula, orbitofrontal cortex (OFC), IPL, postcentral gyrus, precentral gyrus, precuneus, temporal lobe, occipital lobe, thalamus, and cerebellum.

Multi-feature combination analysis results. The results showed that ten combined topological metrics ($r = -0.0061$, $p_{pt} = 0.497$, mean absolute error = 0.55) could not significantly predict the measured CSE scores.

The prediction of personal and relational self-esteem. The leverage centrality of the 46 brain regions could not predict personal self-esteem scores ($r = 0.0265$, $p_{pt} = 0.325$, mean absolute error = 0.32) but significantly predicted relational self-esteem scores ($r = 0.1372$, $p_{pt} = 0.042$, mean absolute error = 0.29). This strongly suggests that the neural basis of CSE is

Please cite this article in press as: Wang G et al. Neural Representation of Collective Self-esteem in Resting-state Functional Connectivity and its Validation in Task-dependent Modality. Neuroscience (2023), https://doi.org/10.1016/j.neuroscience.2023.08.017

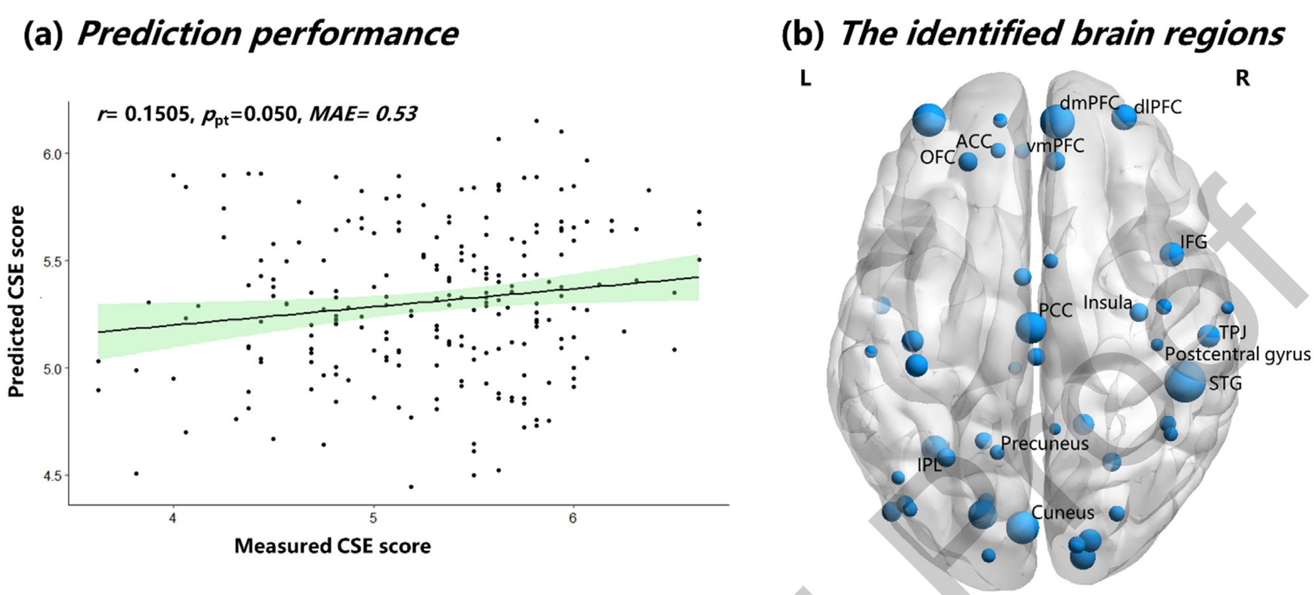

Fig. 3. The association between collective self-esteem questionnaire scores and leverage centrality from the 46 brain regions identified through SVR. (a) Prediction performance (r = 0.1505, p_{pt} = 0.050, mean absolute error = 0.53). The shaded region represents the confidence interval for curve fitting. **(b)** The 46 brain regions were identified as the highest-ranking features in the SVR model (the size indicates their relative weight).

distinct from that of personal self-esteem, and is similar to that of relational self-esteem.

Relevance vector regression results. Similar to the SVR results, RVR analysis found that leverage centrality (r = 0.1933, p_{pt} = 0.007, mean absolute error = 0.51) had excellent prediction performance (Fig. S1 in the supplementary materials); however, nodal betweenness centrality (r = 0.0412, p_{pt} = 0.263, mean absolute error = 0.54), nodal degree centrality (r = 0.0357, p_{pt} = 0.268, mean absolute error = 0.54), nodal efficiency (r = −0.0987, p_{pt} = 0.794, mean absolute error = 0.57), closeness centrality (r = 0.0413, p_{pt} = 0.250, mean absolute error = 0.53), clustering coefficient (r = −0.0113, p_{pt} = 0.475, mean absolute error = 0.53), eigenvector centrality (r = −0.2182, p_{pt} = 0.980, mean absolute error = 0.53), local efficiency (r = −0.0284, p_{pt} = 0.553, mean absolute error = 0.54), shortest path length (r = −0.0786, p_{pt} = 0.759, mean absolute error = 0.55), and subgraph centrality (r = −0.1712, p_{pt} = 0.979, mean absolute error = 0.56) could not significantly predict the measured CSE scores. The regions that were above the threshold were similar to those in the SVR analysis (see Table S1 in the supplementary materials

Validation analysis results from the task-dependent fMRI

Multivariate pattern classification found that the classifiers using activation patterns of the 46 regions from the SVR analysis as features could distinguish collective self-worth from relational self-worth (CR classifier), personal self-worth (CP classifier), and semantic control (CS classifier) conditions. The AUCs of the CS, CP and CR classifiers were 86.68%, 72.52%, and 70.24%, respectively (close to 100% indicates an optimal classification; Fig. 4).

DISCUSSION

The current research attempted to explore the neural basis of CSE from the whole-brain RSFC network. To this end, SVR models were built to predict CSE questionnaire scores using ten topological metrics as features. Further, support vector classification analysis was performed on a task-based fMRI dataset to test the validity of the SVR analysis using the activation patterns of the 46 regions from the SVR analysis as features. The SVR analysis found that leverage centrality successfully decoded individual differences in CSE and the contributing brain regions (e.g., the mPFC, PCC, precuneus, posterior insula, IPL, and TPJ) were distributed across the self-referential processing, affective processing and social cognition networks. Support vector classification analysis found that the activation pattern of the 46 regions distinguished collective self-worth condition from other conditions. This study uncovered the core and distinctive neural basis of CSE in a resting-state fMRI dataset and established the concordance between leverage centrality and the activation pattern (during a collective self-worth task) of the identified regions in terms of representing CSE.

Numerous fMRI studies have reported the neural basis of self-esteem (Pan et al., 2016; Kawamichi et al., 2018; Li et al., 2021; Zeng et al., 2021). The most consistent findings across different modalities for the neural basis of self-esteem converged on the CMS (e.g., the

Table 1. MNI coordinates and weights of the 46 brain regions identified as the highest-ranking features in the SVR model

ROI	MNI coordinate			Weight
	X	*Y*	*Z*	
ACC_pre_L	−11	45	8	0.119
Angular_L	−44	−65	35	0.110
Angular_R	47	−50	29	0.114
Frontal_Sup_Medial_R	9	54	3	0.211
Cerebellum_6_L	−32	−55	−25	0.174
Cingulate_Mid_R	2	−24	30	0.131
Cingulum_Mid_L	0	−15	47	0.196
Cingulum_Post_R	8	−48	31	0.102
Cuneus_L	−16	−77	34	0.183
Cuneus_L	−3	−81	21	0.203
Frontal_Inf_Oper_R	47	10	33	0.162
Frontal_Med_Orb_L	−3	44	−9	0.119
Frontal_Mid_2_L	−34	55	4	0.204
Frontal_Sup_2_L	−10	55	39	0.115
Frontal_Sup_2_R	31	56	14	0.169
Insula_R	36	−9	14	0.135
Lingual_L	−15	−72	−8	0.121
Lingual_L	−16	−52	−1	0.129
Lingual_R	17	−91	−14	0.168
Lingual_R	18	−47	−10	0.149
Lingual_R	27	−59	−9	0.137
Lingual_R	20	−86	−2	0.156
Occipital_Inf_L	−47	−76	−10	0.141
Occipital_Inf_L	15	−87	37	0.128
Occipital_Mid_L	−41	−75	26	0.117
Occipital_Mid_L	−42	−74	0	0.131
Occipital_Mid_R	29	−77	25	0.121
Occipital_Sup_L	−14	−91	31	0.113
OFCant_L	−21	41	−20	0.138
Parietal_Inf_L	−54	−23	43	0.107
Parietal_Inf_L	−28	−58	48	0.136
Postcentral_R	42	−20	55	0.108
Postcentral_R	66	−8	25	0.106
Precentral_L	−40	−19	54	0.151
Precentral_L	−38	−27	69	0.154
Precentral_R	44	−8	57	0.121
Precuneus_L	−11	−56	16	0.117
Rectus_R	8	41	−24	0.139
Supp_Motor_Area_L	−3	2	53	0.131
Supp_Motor_Area_R	7	8	51	0.116
SupraMarginal_R	59	−17	29	0.155
Temporal_Inf_L	−50	−7	−39	0.133
Temporal_Inf_R	46	−47	−17	0.125
Temporal_Sup_R	52	−33	8	0.244
Thalamus	−5	−28	−4	0.111
Thalamus_L	−2	−13	12	0.122

Note: Frontal_Med_Orb is also known as the ventromedial prefrontal cortex (vmPFC); Frontal_Sup_2 is also known as the dorsolateral prefrontal cortex (dlPFC). Angular_L and SupraMarginal_L are also known as the temporoparietal junction gyrus (TPJ). Frontal_Sup_Medial_R is also known as the dorsal medial prefrontal cortex (dmPFC).

mPFC, ACC, and PCC), precuneus, parahippocampal gyrus, insula, dlPFC, OFC, putamen, postcentral gyrus, and temporal lobe, which subserve self-referential processing and affective processing (Leary & Baumeister, 2000; Robins et al., 2001; McClure et al., 2004; Goldberg et al., 2006; Northoff et al., 2006; Levy et al., 2010; Van der Meer et al., 2010; Eisenberger et al., 2011; Feldstein Ewing et al., 2011; Qin & Northoff, 2011; Hughes & Beer, 2012; Herold et al., 2016; Feng et al., 2018a,b; Jiang et al., 2018; Kawamichi et al., 2018; Peng et al., 2019). In line with previous studies, we found that leverage centrality of the abovementioned brain regions significantly predicted CSE. Specifically, the mPFC and ACC were critical for assessing the value of self-related content and conflict monitoring (Eisenberger et al., 2011; Yang et al., 2012; D'Argembeau, 2013). Further, the PCC and precuneus were involved in the retrieval of autobiographical memories (Svoboda et al., 2006; Northoff, 2011; Yaoi et al., 2015; Hu et al., 2016). It has been reported that the

Please cite this article in press as: Wang G et al. Neural Representation of Collective Self-esteem in Resting-state Functional Connectivity and its Validation in Task-dependent Modality. Neuroscience (2023), https://doi.org/10.1016/j.neuroscience.2023.08.017

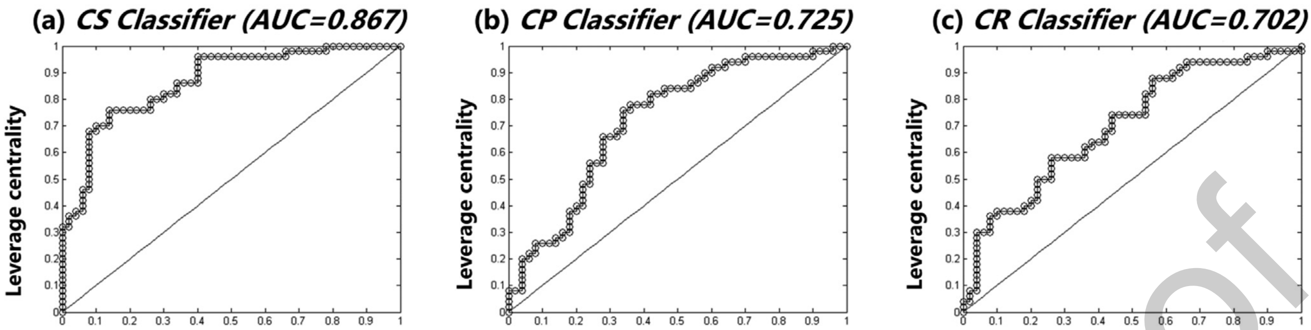

Fig. 4. Classification performance. The three classifiers distinguish collective self-worth from relational self-worth, personal self-worth, and semantic control. CP classifier, distinguished collective self-worth from personal self-worth processing; CR classifier, distinguished collective self-worth from relational self-worth processing; CS classifier, distinguished collective self-worth from semantic processing.

OFC, posterior insula, and postcentral gyrus are engaged in emotional processing during self-worth evaluation (Yang et al., 2016; Izuma et al., 2018).

Moreover, recent research related to relational self-esteem and CSE focused especially on the IPL, TPJ, and IFG, which subserve social cognition processing (Frith & Frith, 2005; Iacoboni & Dapretto, 2006; Blakemore, 2008; Boccadoro et al., 2019; Li et al., 2019; Li et al., 2021; Zeng et al., 2021). These regions contribute to mentalizing and processing social information such as perceiving the attitude of others from a third-person perspective (Premack & Woodruff, 1978; Van Overwalle & Baetens, 2009; Kreifelts et al., 2010). In line with these studies, we found that these regions also contributed to the prediction of CSE questionnaire scores. Overall, our study suggested that the self-referential processing, affective processing, and social cognition networks underlay the neural basis of CSE in the RSFC network.

Membership CSE refers to the personal assessment that her or his group membership is worthwhile (Luhtanen & Crocker, 1992). Private CSE refers to the personal evaluation that the group as a whole is valuable. Importance of identity refers to the degree of importance of self-concept that a person puts on a social group. Because these three components are involved in value assessment and self-reference processing, we cautiously speculated that mPFC, ACC, PCC, and precuneus underlie the neural basis of them. Moreover, value assessment affects an individual's emotions, so the OFC, posterior insula, and postcentral gyrus are related to these components (Leary & Baumeister, 2000; Robins et al., 2001). Public CSE refers to the personal assessment of how others perceive her or his group. It is involved in mentalizing, so the IPL, TPJ, and IFG underlie the neural basis of it. Therefore, there may be correspondence between the core components of CSE and anatomical regions.

The concordance between the leverage centrality from RSFC networks and the activation pattern during a collective self-worth task in terms of representing CSE was studied. The activation pattern of the identified regions from the SVR analysis distinguished collective self-worth from other conditions, proving the validation of the topological properties from RSFC networks in predicting an individual's personality (Tang et al., 2018; Toschi et al., 2018; Kong et al., 2019). CSE has the same neural basis in resting-state fMRI and task-based fMRI paradigms. Moreover, classification accuracy decreased from the CS classifier to the CP classifier and then to the CR classifier. To some extent, this shows that the processing of CSE is quite different from general semantic processing (86.68%). CSE is more easily distinguished from personal self-esteem (72.52%) than relational self-esteem (70.28%). This trend has been found in the prediction of personal and relational self-esteem scores. The leverage centrality of the identified regions could not predict personal self-esteem scores, though it could significantly predict relational self-esteem scores. In addition, shared brain regions (e.g., the IPL, TPJ, and IFG) between CSE and relational self-esteem may lead to this trend. Furthermore, this finding also adds evidence in support of a link between resting-state functional connection and task-based brain activity (Cole et al., 2016; Tavor et al., 2016; Jones et al., 2017; Tobyne et al., 2018; Osher et al., 2019; Cohen et al., 2020; Niu et al., 2021).

Notably, the mPFC underlies the neural basis of CSE. While a previous study did not find that it played a role in representing CSE (Zeng et al., 2021), the leverage centrality of the mPFC contributed to the prediction of CSE scores. We speculated that this may be caused by the distinct analysis methods. In the previous study, contrast and classification analyses were executed. Even if the mPFC participated in the collective self-worth task, these methods may mask its effects. By comparison, in the current study, the leverage centrality of the mPFC was directly used in the prediction. Besides, this discrepancy may also be caused by the distinction between activation level and functional connectivity or the difference between resting-state and task-based fMRI paradigms.

There are some limitations to our study. First, a subjective questionnaire was used to measure CSE. Similar to other questionnaire indices, the CSE scale was inevitably biased by social approval and individual differences in self-awareness (Ellingson et al., 1999). Second, psychological traits that correlate with CSE (e.g., self-efficacy and depression) were not measured nor were they controlled for in the current study. Next, the effect size of the association between nodal leverage

Please cite this article in press as: Wang G et al. Neural Representation of Collective Self-esteem in Resting-state Functional Connectivity and its Validation in Task-dependent Modality. Neuroscience (2023), https://doi.org/10.1016/j.neuroscience.2023.08.017

centrality and collective self-esteem is small. Finally, the experiment only recruited participants from China with a collectivist culture and the number of participants in the task-based fMRI dataset is small. Interpersonal relationships are thought to be more of a concern in collectivist cultures than in individualistic cultures (Yamaguchi et al., 2007). Cross-cultural differences should be considered in future studies that explore the neural basis of CSE.

The current study revealed that self-referential processing (e.g., mPFC, ACC, PCC, precuneus), affective processing (e.g., OFC, posterior insula, postcentral gyrus), and social cognition (e.g., IPL, TPJ, and IFG) networks underlay the neural basis of CSE in the RSFC network. There is concordance between leverage centrality from the RSFC network and the activation pattern elicited during a collective self-worth task in terms of representing CSE. These findings suggest that the RSFC network is as good as task-based activation at revealing the neural basis of CSE.

FUNDING

This research was supported by the National Natural Science Foundation of China [31971019; 32271133], National Key Research and Development Program of China [STI-Major projects: 2022ZD0211000], and Social Science Foundation of Chongqing [2021YC029], China.

OPEN PRACTICES STATEMENT

The data and code that support the findings of this study are available from the corresponding author upon reasonable request, and none of the experiments were preregistered.

CREDIT AUTHORSHIP CONTRIBUTION STATEMENT

Guangtong Wang: Writing – original draft, Writing – review & editing. **Mei Zeng:** Writing – original draft, Writing – review & editing. **Jiwen Li:** Writing – original draft. **Yadong Liu:** Writing – original draft. **Dongtao Wei:** Writing – review & editing. **Zhiliang Long:** . **Haopeng Chen:** Writing – review & editing. **Xinlei Zang:** Writing – review & editing. **Juan Yang:** Writing – original draft.

DECLARATION OF COMPETING INTEREST

The authors declare that they have no known competing financial interests or personal relationships that could have appeared to influence the work reported in this paper.

REFERENCES

Adamovich T, Zakharov I, Tabueva A, Malykh S (2022) The thresholding problem and variability in the EEG graph network parameters. Sci Rep 12(1):18659.

Altinok DCA, Rajkumar R, Nießen D, Sbaihat H, Kersey M, Shah NJ, Neuner I (2021) Common neurobiological correlates of resilience and personality traits within the triple resting-state brain networks assessed by 7-Tesla ultra-high field MRI. Sci Rep 11(1):1–15.

Bettencourt BA, Charlton K, Eubanks J, Kernahan C, Fuller B (1999) Development of collective self-esteem among students: Predicting adjustment to college. Basic Appl Soc Psychol 21 (3):213–222.

Biswal B, Zerrin Yetkin F, Haughton VM, Hyde JS (1995) Functional connectivity in the motor cortex of resting human brain using echo-planar MRI. Magn Reson Med 34(4):537–541.

Blakemore SJ (2008) The social brain in adolescence. Nat Rev Neurosci 9(4):267–277.

Boccadoro S, Cracco E, Hudson AR, Bardi L, Nijhof AD, Wiersema JR, Mueller SC (2019) Defining the neural correlates of spontaneous theory of mind (ToM): An fMRI multi-study investigation. Neuroimage 203 116193.

Boccaletti S, Latora V, Moreno Y, Chavez M, Hwang DU (2006) Complex networks: Structure and dynamics. Phys Rep 424(4–5):175–308.

Bonacich P (2007) Some unique properties of eigenvector centrality. Soc Networks 29(4):555–564.

Brereton RG, Lloyd GR (2010) Support vector machines for classification and regression. Analyst 135(2):230–267.

Bullmore E, Sporns O (2009) Complex brain networks: graph theoretical analysis of structural and functional systems. Nat Rev Neurosci 10(3):186–198.

Cao H, Plichta MM, Schäfer A, Haddad L, Grimm O, Schneider M, Tost H (2014) Test-retest reliability of fMRI-based graph-theoretical properties during working memory, emotion processing, and resting state. Neuroimage 84:888–900.

Cawley GC, Talbot NL (2004) Fast exact leave-one-out cross-validation of sparse least-squares support vector machines. Neural Netw 17(10):1467–1475.

Chavez RS, Heatherton TF (2015) Multimodal frontostriatal connectivity underlies individual differences in self-esteem. Social Cogn Affect Neurosci 10(3):364–370. https://doi.org/10.1093/scan/nsu063.

Chen G, Chen G, Xie C, Li SJ (2011) Negative functional connectivity and its dependence on the shortest path length of positive network in the resting-state human brain. Brain Connect 1 (3):195–206.

Chen H, Zhao X, Zeng M, Li J, Ren X, Zhang M, Yang J (2021a) Collective self-esteem and perceived stress among the non-infected general public in China during the 2019 coronavirus pandemic: A multiple mediation model. Pers Individ Differ 168 110308.

Chen X, Huang Y, Xiao M, Luo YJ, Liu Y, Song S, Chen H (2021b) Self and the brain: Self-concept mediates the effect of resting-state brain activity and connectivity on self-esteem in school-aged children. Pers Individ Differ 168 110287.

Chow TE, Westphal AJ, Rissman J (2018) Multi-voxel pattern classification differentiates personally experienced event memories from secondhand event knowledge. Neuroimage 176:110–123.

Cohen AD, Chen Z, Parker Jones O, Niu C, Wang Y (2020) Regression-based machine-learning approaches to predict task activation using resting-state fMRI. Hum Brain Mapp 41 (3):815–826.

Cole MW, Ito T, Bassett DS, Schultz DH (2016) Activity flow over resting-state networks shapes cognitive task activations. Nat Neurosci 19(12):1718–1726.

Crocker J, Major B (1989) Social stigma and self-esteem: The self-protective properties of stigma. Psychol Rev 96(4):608.

Crocker J, Luhtanen R, Blaine B, Broadnax S (1994) Collective self-esteem and psychological well-being among White, Black, and Asian college students. Pers Soc Psychol Bull 20(5):503–513.

Cui Z, Su M, Li L, Shu H, Gong G (2018) Individualized prediction of reading comprehension ability using gray matter volume. Cereb Cortex 28:1656–1672. https://doi.org/10.1093/cercor/bhx061.

Cui Z, Gong G (2018) The effect of machine learning regression algorithms and sample size on individualized behavioral prediction with functional connectivity features. Neuroimage 178:622–637.

D'Argembeau A (2013) On the role of the ventromedial prefrontal cortex in self-processing: the valuation hypothesis. Front Hum Neurosci 7:372.

Deng Z, Chandrasekaran B, Wang S, Wong PC (2016) Resting-state low-frequency fluctuations reflect individual differences in spoken language learning. Cortex 76:63–78.

Dimitriadis SI, Salis C, Tarnanas I, Linden DE (2017) Topological filtering of dynamic functional brain networks unfolds informative chronnectomics: a novel data-driven thresholding scheme based on orthogonal minimal spanning trees (OMSTs). Front Neuroinf 11:28.

Dosenbach NU, Nardos B, Cohen AL, Fair DA, Power JD, Church JA, Schlaggar BL (2010) Prediction of individual brain maturity using fMRI. Science 329(5997):1358–1361.

Du HF, King RB, Chi PL (2012) The development and validation of the relational self-esteem scale. Scand J Psychol 53(3):258–264. https://doi.org/10.1111/j.1467-9450.2012.00946.x.

Du H, King RB, Chi P (2017) Self-esteem and subjective well-being revisited: The roles of personal, relational, and collective self-esteem. PLoS One 12(8):e0183958.

Dubois J, Galdi P, Han Y, Paul LK, Adolphs R (2018) Resting-state functional brain connectivity best predicts the personality dimension of openness to experience. Pers Neurosci 1.

Ecker C, Marquand A, Mourão-Miranda J, Johnston P, Daly EM, Brammer MJ, Murphy DG (2010) Describing the brain in autism in five dimensions- magnetic resonance imaging-assisted diagnosis of autism spectrum disorder using a multiparameter classification approach. J Neurosci 30(32):10612–10623.

Eisenberger NI, Inagaki TK, Muscatell KA, Byrne Haltom KE, Leary MR (2011) The neural sociometer: brain mechanisms underlying state self-esteem. J Cogn Neurosci 23(11):3448–3455.

Ellingson JE, Sackett PR, Hough LM (1999) Social desirability corrections in personality measurement: Issues of applicant comparison and construct validity. J Appl Psychol 84 (2):155–166. https://doi.org/10.1037/0021-9010.84.2.155.

Estrada E, Rodriguez-Velazquez JA (2005) Subgraph centrality in complex networks. *Phys* Rev E 71(5) 056103.

Feldstein Ewing SW, Filbey FM, Sabbineni A, Chandler LD, Hutchison KE (2011) How psychosocial alcohol interventions work: A preliminary look at what fMRI can tell us. Alcohol Clin Exp Res 35(4):643–651.

Feng C, Yan X, Huang W, Han S, Ma Y (2018a) Neural representations of the multidimensional self in the cortical midline structures. Neuroimage 183:291–299. https://doi.org/10.1016/j.neuroimage.2018.08.018.

Feng C, Zhu Z, Gu R, Wu X, Luo YJ, Krueger F (2018b) Resting-state functional connectivity underlying costly punishment: a machine-learning approach. Neuroscience 385:25–37.

Finn ES, Shen X, Scheinost D, Rosenberg MD, Huang J, Chun MM, Constable RT (2015) Functional connectome fingerprinting: identifying individuals using patterns of brain connectivity. Nat Neurosci 18(11):1664–1671.

Freeman LC (1978) Centrality in social networks conceptual clarification. Soc Networks 1(3):215–239.

Frith C, Frith U (2005) Theory of mind. *Curr Biol* 15(17):R644–R645.

Furr RM (2009) Personality psychology as a truly behavioural science. Eur J Pers 23(5):369–401.

Goldberg II, Harel M, Malach R (2006) When the brain loses its self: prefrontal inactivation during sensorimotor processing. Neuron 50 (2):329–339.

Hassan G, Rousseau C, Moreau N (2013) Ethnic and religious discrimination: The multifaceted role of religiosity and collective self-esteem. Transcult Psychiatry 50(4):475–492.

Haxby JV, Gobbini MI, Furey ML, Ishai A, Schouten JL, Pietrini P (2001) Distributed and overlapping representations of faces and objects in ventral temporal cortex. Science 293 (5539):2425–2430.

He L, Wei D, Yang F, Zhang J, Cheng W, Feng J, Qiu J (2021) Functional connectome prediction of anxiety related to the COVID-19 pandemic. Am J Psychiatry 178(6):530–540.

He Y, Evans A (2010) Graph theoretical modeling of brain connectivity. Curr Opin Neurol 23(4):341–350.

Herold D, Spengler S, Sajonz B, Usnich T, Bermpohl F (2016) Common and distinct networks for self-referential and social stimulus processing in the human brain. Brain Structure Function 221(7):3475–3485. https://doi.org/10.1007/s0 0429- 015-1113-9.

Hojjati SH, Ebrahimzadeh A, Khazaee A, Babajani-Feremi A, Alzheimer's Disease Neuroimaging Initiative (2017) Predicting conversion from MCI to AD using resting-state fMRI, graph theoretical approach and SVM. J Neurosci Methods 282:69–80.

Hu C, Di X, Eickhoff SB, Zhang M, Peng K, Guo H, Sui J (2016) Distinct and common aspects of physical and psychological self-representation in the brain: a meta-analysis of self-bias in facial and self-referential judgements. Neurosci Biobehav Rev 61:197–207.

Hughes BL, Beer JS (2012) Orbitofrontal cortex and anterior cingulate cortex are modulated by motivated social cognition. Cereb Cortex 22(6):1372–1381.

Iacoboni M, Dapretto M (2006) The mirror neuron system and the consequences of its dysfunction. Nat Rev Neurosci 7 (12):942–951.

Izuma K, Kennedy K, Fitzjohn A, Sedikides C, Shibata K (2018) Neural activity in the reward-related brain regions predicts implicit self-esteem: A novel validity test of psychological measures using neuroimaging. J Pers Soc Psychol 114(3):343.

Jaccard JJ (1974) Predicting social behavior from personality traits. J Res Pers 7(4):358–367.

James W, Burkhardt F, Bowers F, Skrupskelis IK (1890). The principles of psychology, vol. 1, No. 2. London: Macmillan.

Jia XJ (2009) The Revision of the collective self-esteem scale for college students. China J. Health Psychol 17:288–290.

Jiang K, Wu S, Shi Z, Liu M, Peng M, Shen Y, Yang J (2018) Activations of the dorsolateral prefrontal cortex and thalamus during agentic self-evaluation are negatively associated with trait self-esteem. Brain Res 1692:134–141.

Jimura K, Poldrack RA (2012) Analyses of regional-average activation and multivoxel pattern information tell complementary stories. Neuropsychologia 50(4):544–552.

Jones OP, Voets NL, Adcock JE, Stacey R, Jbabdi S (2017) Resting connectivity predicts task activation in pre-surgical populations. NeuroImage: Clinical 13:378–385.

Joyce KE, Laurienti PJ, Burdette JH, Hayasaka S (2010) A new measure of centrality for brain networks. PLoS One 5(8):e12200.

Kaplan JT, Man K, Greening SG (2015) Multivariate cross-classification: applying machine learning techniques to characterize abstraction in neural representations. Front Hum Neurosci 9:151.

Kashyap R, Kong R, Bhattacharjee S, Li J, Zhou J, Yeo BT (2019) Individual-specific fMRI-Subspaces improve functional connectivity prediction of behavior. Neuroimage 189:804–812.

Kawamichi H, Sugawara SK, Hamano YH, Kitada R, Nakagawa E, Kochiyama T, Sadato N (2018) Neural correlates underlying change in state self-esteem. Sci Rep 8(1):1–14.

Kong R, Li J, Orban C, Sabuncu MR, Liu H, Schaefer A, Yeo BT (2019) Spatial topography of individual-specific cortical networks predicts human cognition, personality, and emotion. Cereb Cortex 29(6):2533–2551.

Kreifelts B, Ethofer T, Huberle E, Grodd W, Wildgruber D (2010) Association of trait emotional intelligence and individual fMRI-activation patterns during the perception of social signals from voice and face. Hum Brain Mapp 31(7):979–991.

Krienen FM, Yeo BT, Buckner RL (2014) Reconfigurable task-dependent functional coupling modes cluster around a core functional architecture. Philos Trans R Soc, B 369 (1653):20130526.

Lacosse E, Scheffler K, Lohmann G, Martius G (2021) Jumping over baselines with new methods to predict activation maps from resting-state fMRI. Sci Rep 11(1):1–15.

Latora V, Marchiori M (2001) Efficient behavior of small-world networks. Phys Rev Lett 87(19) 198701.

Leary MR, Baumeister RF (2000) The nature and function of self-esteem: Sociometer theory. Adv Exp Soc Psychol 32:1–62.

Levy I, Snell J, Nelson AJ, Rustichini A, Glimcher PW (2010) Neural representation of subjective value under risk and ambiguity. J Neurophysiol 103(2):1036–1047.

Li J, Liu M, Peng M, Jiang K, Chen H, Yang J (2019) Positive representation of relational self-esteem versus personal self-esteem in Chinese with interdependent self-construal. Neuropsychologia 134 107195.

Li J, Zeng M, Liu M, Zhao X, Hu W, Wang C, Yang J (2021) Multivariable pattern classification differentiates relational self-esteem from personal self-esteem. Soc Cogn Affect Neurosci 16 (7):726–735.

Li Z, Chen R, Guan M, Wang E, Qian T, Zhao C, Li Y (2018) Disrupted brain network topology in chronic insomnia disorder: a resting-state fMRI study. NeuroImage: Clinical 18:178–185.

Liu F, Xie B, Wang Y, et al. (2015) Characterization of post-traumatic stress disorder using resting-state fMRI with a multi-level parametric classification approach. Brain Topogr 28(2):221–237.

Liu J, Xia M, Dai Z, Wang X, Liao X, Bi Y, He Y (2017) Intrinsic brain hub connectivity underlies individual differences in spatial working memory. Cereb Cortex 27(12):5496–5508.

Liu W, Kohn N, Fernández G (2019) Intersubject similarity of personality is associated with intersubject similarity of brain connectivity patterns. Neuroimage 186:56–69.

Luhtanen R, Crocker J (1992) A collective self-esteem scale: Self-evaluation of one's social identity. Pers Soc Psychol Bull 18 (3):302–318.

McClure SM, Laibson DI, Loewenstein G, Cohen JD (2004) Separate neural systems value immediate and delayed monetary rewards. Science 306(5695):503–507.

Neiss MB, Sedikides C, Stevenson J (2002) Self-esteem: a behavioural genetic perspective. Eur J Pers 16(5):351–367.

Niu C, Cohen AD, Wen X, Chen Z, Lin P, Liu X, Zhang M (2021) Modeling motor task activation from resting-state fMRI using machine learning in individual subjects. Brain Imaging Behav 15 (1):122–132.

Noble S, Spann MN, Tokoglu F, Shen X, Constable RT, Scheinost D (2017) Influences on the test–retest reliability of functional connectivity MRI and its relationship with behavioral utility. Cereb Cortex 27(11):5415–5429.

Northoff G (2011) Self and brain: what is self-related processing? Trends Cogn Sci 15(5):186–187.

Northoff G, Heinzel A, De Greck M, Bermpohl F, Dobrowolny H, Panksepp J (2006) Self-referential processing in our brain—a meta-analysis of imaging studies on the self. Neuroimage 31 (1):440–457.

Nostro AD, Müller VI, Varikuti DP, Pläschke RN, Hoffstaedter F, Langner R, Eickhoff SB (2018) Predicting personality from network-based resting-state functional connectivity. Brain Struct Funct 223(6):2699–2719.

Okamoto K, Chen W, Li XY (2008) Ranking of closeness centrality for large-scale social networks. Lect Notes Comput Sci 5059:186–195.

Onoda K, Yamaguchi S (2015) Dissociative contributions of the anterior cingulate cortex to apathy and depression: topological evidence from resting-state functional MRI. Neuropsychologia 77:10–18.

Osher DE, Brissenden JA, Somers DC (2019) Predicting an individual's dorsal attention network activity from functional connectivity fingerprints. J Neurophysiol 122(1):232–240.

Pan W, Liu C, Yang Q, Gu Y, Yin S, Chen A (2016) The neural basis of trait self-esteem revealed by the amplitude of low-frequency fluctuations and resting state functional connectivity. Soc Cogn Affect Neurosci 11(3):367–376.

Passamonti L, Riccelli R, Indovina I, Duggento A, Terracciano A, Toschi N (2019) Time-resolved connectome of the five-factor model of personality. Sci Rep 9(1):1–12.

Peng M, Wu S, Shi Z, Jiang K, Shen Y, Dedovic K, Yang J (2019) Brain regions in response to character feedback associated with the state self-esteem. Biol Psychol 148 107734.

Power JD, Cohen AL, Nelson SM, Wig GS, Barnes KA, Church JA, Petersen SE (2011) Functional network organization of the human brain. Neuron 72(4):665–678.

Premack D, Woodruff G (1978) Does the chimpanzee have a theory of mind? Behav Brain Sci 1(4):515–526.

Qin P, Northoff G (2011) How is our self-related to midline regions and the default-mode network? Neuroimage 57(3):1221–1233.

Robins RW, Hendin HM, Trzesniewski KH (2001) Measuring global self-esteem: Construct validation of a single-item measure and the Rosenberg self-esteem scale. Pers Soc Psychol Bull 27 (2):151–161. https://doi.org/10.1177/0146167201272002.

Rosenberg M (1965) Rosenberg self-esteem scale (RSE). Acceptance and commitment therapy. Meas Package 61(52):18.

Sapountzis P, Schluppeck D, Bowtell R, Peirce JW (2010) A comparison of fMRI adaptation and multivariate pattern classification analysis in visual cortex. Neuroimage 49 (2):1632–1640.

Saramäki J, Kivelä M, Onnela JP, Kaski K, Kertesz J (2007) Generalizations of the clustering coefficient to weighted complex networks. Phys Rev E 75(2) 027105.

Schaefer A, Kong R, Gordon EM, Laumann TO, Zuo XN, Holmes AJ, Yeo BT (2018) Local-global parcellation of the human cerebral cortex from intrinsic functional connectivity MRI. Cereb Cortex 28 (9):3095–3114.

Song J, Nair VA, Gaggl W, Prabhakaran V (2015) Disrupted brain functional organization in epilepsy revealed by graph theory analysis. Brain Connect 5(5):276–283.

Svoboda E, McKinnon MC, Levine B (2006) The functional neuroanatomy of autobiographical memory: a meta-analysis. Neuropsychologia 44(12):2189–2208.

Tang H, Lu X, Cui Z, Feng C, Lin Q, Cui X, Liu C (2018) Resting-state functional connectivity and deception: exploring individualized deceptive propensity by machine learning. Neuroscience 395:101–112.

Tang Y, Jiang W, Liao J, Wang W, Luo A (2013) Identifying individuals with antisocial personality disorder using resting-state FMRI. PLoS One 8(4):e60652.

Tavor I, Jones OP, Mars RB, Smith SM, Behrens TE, Jbabdi S (2016) Task-free MRI predicts individual differences in brain activity during task performance. Science 352(6282):216–220.

Tipping ME (2001) Sparse Bayesian learning and the relevance vector machine. J Mach Learn Res 1(Jun):211–244.

Tobyne SM, Somers DC, Brissenden JA, Michalka SW, Noyce AL, Osher DE (2018) Prediction of individualized task activation in sensory modality-selective frontal cortex with 'connectome fingerprinting'. Neuroimage 183:173–185.

Toschi N, Riccelli R, Indovina I, Terracciano A, Passamonti L (2018) Functional connectome of the five-factor model of personality. Pers Neurosci 1.

Uehara T, Yamasaki T, Okamoto T, Koike T, Kan S, Miyauchi S, Tobimatsu S (2014) Efficiency of a "small-world" brain network depends on consciousness level: a resting-state fMRI study. Cereb Cortex 24(6):1529–1539.

Van der Meer L, Costafreda S, Aleman A, David AS (2010) Self-reflection and the brain: a theoretical review and meta-analysis of neuroimaging studies with implications for schizophrenia. Neurosci Biobehav Rev 34(6):935–946.

Van Overwalle F, Baetens K (2009) Understanding others' actions and goals by mirror and mentalizing systems: a meta-analysis. Neuroimage 48(3):564–584.

Vilares I, Wesley MJ, Ahn WY, et al. (2017) Predicting the knowledge–recklessness distinction in the human brain. Proc Natl Acad Sci USA 114(12):3222–3227.

Wang X, Lin Q, Xia M, He Y (2018) Differentially categorized structural brain hubs are involved in different microstructural, functional, and cognitive characteristics and contribute to individual identification. Hum Brain Mapp 39(4):1647–1663.

Wang J, Wang X, Xia M, Liao X, Evans A, He Y (2015) GRETNA: a graph theoretical network analysis toolbox for imaging connectomics. Front Hum Neurosci 9:386.

Weaverdyck ME, Lieberman MD, Parkinson C (2020) Tools of the Trade Multivoxel pattern analysis in fMRI: a practical introduction for social and affective neuroscientists. Soc Cogn Affect Neurosci 15(4):487–509.

Woo CW, Chang LJ, Lindquist MA, Wager TD (2017) Building better biomarkers: brain models in translational neuroimaging. Nat Neurosci 20(3):365–377.

Yamaguchi S, Greenwald AG, Banaji MR, Murakami F, Chen D, Shiomura K, Kobayashi C, Cai H, Krendl A (2007) Apparent universality of positive implicit self-esteem. Psychol Sci 18 (6):498–500. https://doi.org/10.1111/j.1467-9280.2007.01928.x.

Yan C, Zang Y (2010) DPARSF: a MATLAB toolbox for“ pipeline” data analysis of resting-state fMRI. Front Syst Neurosci 4:13.

Yang J, Dedovic K, Chen W, Zhang Q (2012) Self-esteem modulates dorsal anterior cingulate cortical response in self-referential processing. Neuropsychologia 50(7):1267–1270.

Yang J, Xu X, Chen Y, Shi Z, Han S (2016) Trait self-esteem and neural activities related to self-evaluation and social feedback. Sci Rep 6(1):1–10.

Yaoi K, Osaka M, Osaka N (2015) Neural correlates of the self-reference effect: evidence from evaluation and recognition processes. Front Hum Neurosci 9:383.

Zeng M, Li J, Wang C, Deng C, Li R, Chen H, Yang J (2021) Neural processing of personal, relational, and collective self-worth reflected individual differences of self-esteem. J Pers 00:1–19.

Zuo X-N, Xing X-X (2014) Test-retest reliabilities of resting-state fmri measurements in human brain functional connectomics: a systems neuroscience perspective. Neurosci Biobehav Rev 45:100–118. https://doi.org/10.1016/j.neubiorev.2014.05.009.

Zuo XN, Di Martino A, Kelly C, Shehzad ZE, Gee DG, Klein DF, Milham MP (2010) The oscillating brain: complex and reliable. Neuroimage 49(2):1432–1445.

APPENDIX A. SUPPLEMENTARY MATERIAL

Supplementary material to this article can be found online at https://doi.org/10.1016/j.neuroscience.2023.08.017.

(Received 14 February 2023, Accepted 9 August 2023)
(Available online xxxx)